Research Article

Yang He*, Chunlin Chen, and Xiaodong Yang

Thermodynamic analysis of vanadium distribution behavior in blast furnaces and basic oxygen furnaces

https://doi.org/10.1515/htmp-2022-0259 received September 06, 2022; accepted November 30, 2022

Abstract: Production data from a vanadium (V)-containing titaniferous magnetite (VTM) smelting blast furnace (BF) ironmaking plant and a V-recovering basic oxygen furnace (BOF) shop were collected over a period of 1 year. The corresponding thermodynamics was analyzed in terms of V reduction in the BF operation and V oxidation in the BOF operation. The thermodynamic calculations were performed using the software Multi-Phase Equilibrium (MPE), in which generalized central atom model was introduced into the description of molten slag and applied for the slag database. The effects of operating conditions on V distribution ratios between slag and hot metal/semi-steel were analyzed and compared with the plant data. The simulated results could reproduce the variation of V distribution ratios with slag temperature and composition and provide the guidance for operators to control V distribution behavior for the better process operation.

Keywords: V-containing titaniferous magnetite, blast furnace, basic oxygen furnace, V distribution ratio, GCA model

Xiaodong Yang: Institute of Engineering Technology, University of Science and Technology Beijing, Beijing 100083, People's Republic of China; Pangang Group Xichang Steel & Vanadium Co. Ltd, Xichang, Sichuan 615000, People's Republic of China ORCID: Yang He 0000-0002-5242-9293

1 Introduction

Vanadium (V), one of the key alloying elements in the steel industry, is widely distributed in the Earth's crust with an average content of 0.02%. According to the statistics, more than 80% of the produced V metal are extracted from V-containing titaniferous magnetite (VTM) worldwide. In China, the VTM in Panzhihua-Xichang and Chengde regions is not only the source of iron ore but also the main raw material for V extraction [1,2]. The main route for extracting V from VTM has three stages [3,4]. At Stage 1, V in VTM is reduced into hot metal in blast furnace (BF) operation. The V-containing hot metal is oxidized to make a V-rich slag and semi-steel in basic oxygen furnace (BOF) at Stage 2. V is extracted from the V-rich slag through hydrometallurgy at Stage 3. In order to maximize V extraction, it is of great importance to develop a greater understanding of V distribution behavior between slag and hot metal/semisteel in the BF and BOF operations.

Over the past few decades, some scholars have investigated V distribution behavior for multi-component V-containing slags equilibrated with molten steel or hot metal. V distribution ratios were measured for CaO–MgO–FeO $_x$ –SiO $_2$ slags and molten steel by Inoue and Suito [5] and Selin [6], CaO–SiO $_2$ –MgO–Al $_2$ O $_3$ slags and molten steel by Shin et al. [7], CaO–SiO $_2$ –Al $_2$ O $_3$ –MgO–TiO $_2$ slags and hot metal by Andersson et al. [8], and CaO–SiO $_2$ –Al $_2$ O $_3$ –MgO–TiO $_2$ –V $_2$ O $_3$ slags and hot metal by Wang et al. [9]. However, the limited experimental data are insufficient to understand the complex molten slag–metal reactions, and none of these studies could give the well-accepted correlation for V distribution behavior between slag and hot metal/molten steel in terms of composition and temperature.

For the purpose of understanding the slag-metal reactions more fully within the limited experimental data, the thermodynamic model based on the accurate database, known as the Calphad method, has been developed in recent years based on the reliable published thermodynamic data [10]. Generalized central atom (GCA) model,

^{*} Corresponding author: Yang He, Institute of Engineering
Technology, University of Science and Technology Beijing, Beijing
100083, People's Republic of China; CSIRO Mineral Resources,
Clayton, Victoria 3168, Australia, e-mail: heyang2020@ustb.edu.cn
Chunlin Chen: CSIRO Mineral Resources, Clayton, Victoria 3168,
Australia

jointly developed by ArcelorMittal and the Commonwealth Scientific and Industrial Research Organisation (CSIRO), was one of the recent progresses in this domain [11–14]. GCA model is derived from central atom (CA) model and Cell Model. On the one hand, GCA model continues the basic concept of CA model by describing liquid structure with a central atom and its nearest neighbors, but GCA model extends to cover molten oxides. On the other hand, GCA model has the same types of model parameters, cell formation energy, and cell interaction energy, with Cell Model, and GCA model completely inherits the binary parameters of Cell Model. The recent collaborative research between ArcelorMittal and CSIRO has assessed GCA model parameters for V-containing slags in the system of SiO₂-A l_2O_3 -FeO_x-MnO-MgO-CaO-Na₂O-K₂O-P₂O₅-TiO_x-CrO_x-VO_x-S-CaF₂, and the slag database has been implemented in the thermodynamic package called Multi-Phase Equilibrium software for the thermodynamic calculation of metallurgical systems.

Considering the high temperature, high pressure, and intense smelting conditions of BF and BOF operations, the slag and hot metal/semi-steel phases are believed to be close to reach equilibrium in BF hearths and BOF converters, and thus, the pyrometallurgy process could be simulated by the thermodynamic model. In the present study, GCA model was used to study V distribution behavior between slag and hot metal/semi-steel. Production data from a VTM smelting BF ironmaking plant and a V-recovering BOF shop were collected over a period of 1 year. The simulated results were compared with the plant measurements and provided the guidance for operators to control V distribution ratios for the better process operation.

2 GCA model

The detailed introduction of GCA model can be found in the previous studies [11–14]. The general description of this model is given in the following.

GCA model describes the liquid structure in terms of cells composed of a central atom and its shell of nearest neighbors. Around the central atom, there are neighboring atoms on the cationic and anionic shells, respectively. In a multi-component system, the cell is shown as

i_1, i_2, i_k, i_t	Atoms on cationic shell
J	Central atom
$j_{t+1}, j_r,,j_m$	Atoms on anionic shell

Instead of the pair interaction in Cell Model, GCA model considers the interaction between the central atom and its neighbors and thus provides a better description of short-range ordering phenomenon in liquid phase.

In a similar way to Cell Model, the network-breaking reaction in GCA model can be represented as follows:

$$\frac{1}{2}(k-J-k) + \frac{1}{2}(l-J-l) \to k-J-l, \tag{1}$$

where J represents the central atom, and k and l represent the neighboring atoms. The total energy of a cell is written with two sets of parameters: the cell formation energy φ_{kl}^J and the cell interaction energy E_{kl}^J . For the metallurgical slags, both φ_{kl}^J and E_{kl}^J are inherited from Cell Model, but more sophisticated and flexible interaction parameter terms can be introduced into the GCA model to overcome the limitation of Cell Model.

During the database development, the parameters of the formation energy and interaction energy are assumed to have a linear variation with the composition:

$$\varphi_{kl}^{J} = {}^{0}\varphi_{kl}^{J} + {}^{1}\varphi_{kl}^{J} \cdot x_{k}, \tag{2}$$

$$E_{kl}^{J} = {}^{0}E_{kl}^{J} + {}^{1}E_{kl}^{J} \cdot x_{k}, \tag{3}$$

where x_k is the mole fraction of cations #k. The formation energy parameters $({}^0\varphi_{kl}^J, {}^1\varphi_{kl}^J)$ and interaction energy parameters $({}^0E_{kl}^J, {}^1E_{kl}^J)$ are optimized against the published thermodynamic data of the target system.

3 Evaluation of GCA model

Before applying in the thermodynamic analysis of V distribution behavior in BF and BOF, the GCA model was evaluated by comparing the calculated V activities in V-containing slags with the published experimental measurements. The V activities in multi-component V-containing slags have been investigated in a number of studies [5–9,15], which are summarized in Table 1. These slags within the system of CaO–SiO₂–MgO–FeO_x–Al₂O₃–TiO₂–VO_x were in equilibrium with hot metal, molten steel, or solid platinum metal. Except that the slag in Dong et al.'s study [15] was equilibrated with a CO–CO₂–Ar gas mixture with fixed oxygen partial pressure, the slags in the other studies [5–9] are saturated with metal iron. Thus, the oxygen potential in the slags is expected to be low, and V in the slags should exist as V³⁺ dominantly.

The $VO_{1.5}$ activity (solid $VO_{1.5}$ standard state) in slag was calculated according to the following reaction [15]:

References	Temperature (°C)	Slag system	Metal
Inoue and Suito [5]	1,550-1,650	CaO-SiO ₂ -MgO-FeO _x -VO _x	Fe-V
Selin [6]	1,600	$CaO-SiO_2-MgO-FeO_x-VO_x$	Fe-V
Shin et al. [7]	1,600-1,700	$CaO-SiO_2-MgO-FeO_x-Al_2O_3-VO_x$	Fe-V
Andersson et al. [8]	1,450-1,500	$CaO-SiO_2-MgO-Al_2O_3-TiO_2-VO_x$	Fe-C-V
Wang et al. [9]	1,500	$CaO-SiO_2-MgO-Al_2O_3-TiO_2-VO_x$	Fe-C-V
Dong et al. [15]	1,530-1,650	$CaO-SiO_2-MgO-Al_2O_3-VO_x$	Pt-V

Table 1: Summary of the published studies of the multi-component V-containing slags

$$V_{(s)} + \frac{3}{4}O_2 = VO_{1.5(s)},$$
 (4)

$$\Delta G^{\theta} = -600,405 + 112.97T (J \cdot mol^{-1}).$$

The $VO_{1.5}$ activity was related to the V activity, the oxygen potential, and the Gibbs energy of the reaction. The V activity and the oxygen potential in the published studies could be determined based on their corresponding experimental conditions.

Inoue and Suito [5] investigated the V distribution between CaO-SiO₂-MgO-FeO_x slag and molten steel in the temperature range of 1,550–1,650°C. Selin [6] measured the MgO solubility in CaO-SiO₂-MgO-FeO_x slag and the V distribution between MgO-saturated slag and molten steel at 1,600°C. Both reported the slag composition and the V and O contents in molten steel after equilibration. Considering the V in metal is less than 100 ppm, the V activity (1 wt% V in metal as standard state) can be approximated to be the V content in metal. The interconversion of V activity in the standard states of solid V and 1 wt% V in metal was based on the following reaction [16]:

$$V_{(s)} = [V],$$
 (5)
$$\Delta G^{\theta} = -20710 - 45.6T (J \cdot mol^{-1}).$$

The oxygen potential of the system was determined according to the measured oxygen content in molten steel. The O content measured in molten steel was less than 0.2 wt%, and the calculation using the steel alloy model showed that O activity (1 wt% O in metal as standard state) can be approximated to be the weight percentage of O in molten steel. The measured O content/activity was converted to oxygen partial pressure by the following reaction [16]:

$$\frac{1}{2}O_{2(g)} = [O],$$

$$\Delta G^{\theta} = -117,150 - 2.89T (J \cdot mol^{-1}).$$
(6)

Figure 1 shows the comparison of the oxygen partial pressure $p(O_2)$ calculated based on the [Fe]/(FeO) equilibrium between slag and metal with the measured O content

in the metal. The good agreement between the model calculation and experimental data confirms that the slag and metal are very close to the equilibrium.

Shin et al. [7] studied the equilibrium distribution of V between $\text{CaO-SiO}_2\text{-MgO-FeO}_x\text{-Al}_2\text{O}_3$ slag with different basicities and molten steel under an inert atmosphere in the temperature range of 1,600–1,700°C. Only the V content was reported in molten steel. The V activity (1 wt% V in metal as standard state) was approximated to be the V content in molten steel, and the oxygen potential could only be calculated based on the [Fe]/(FeO) equilibrium. However, the FeO content in slag was only 1–2 wt%, and the calculated oxygen potential was expected to have high uncertainty.

Andersson et al. [8] investigated the V distribution between $CaO-SiO_2-MgO-Al_2O_3-TiO_2$ slag and C saturated hot metal tapped from a commercial BF. Wang et al. [9] measured the V distribution between $CaO-SiO_2-MgO-Al_2O_3-TiO_2$ slag with 57 wt% TiO_2 and C saturated hot metal. Both reported the detailed compositions of slag and hot metal. The V activity (1 wt% V in metal as standard state) was calculated using Wagner's

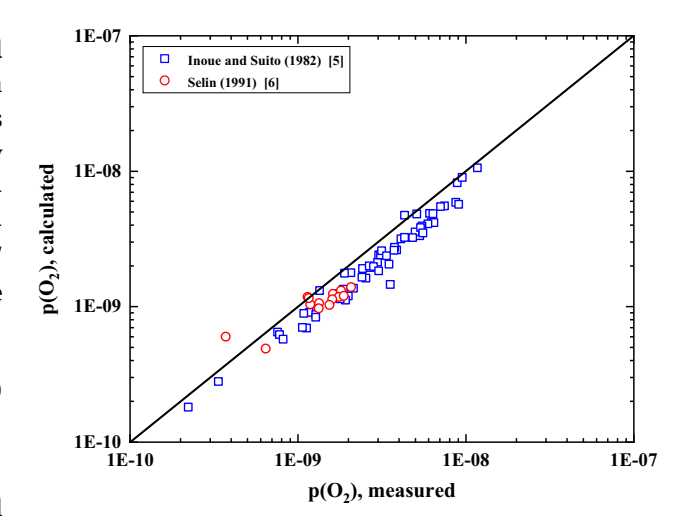


Figure 1: Comparison of the calculated oxygen particle pressure $p(O_2)$ with the experimental measurements [5,6].

formalism. Although the O content in hot metal was not reported, the oxygen potential could be calculated based on the $[Si]/(SiO_2)$ equilibrium. The Si activity (1 wt% Si in metal as standard state) was calculated using Wagner's formalism as well. The interconversion of Si activity in the standard states of liquid Si and 1 wt% Si in metal was based on the following reaction [16]:

$$Si_{(l)} = [Si],$$
 (7)
$$\Delta G^{\theta} = -131,500 - 17.16T (J \cdot mol^{-1}).$$

Dong et al. [15] equilibrated $CaO-SiO_2-MgO-Al_2O_3-VO_x$ slag with solid platinum metal under a $CO-CO_2-Ar$ gas mixture at the temperatures of 1,530, 1,600, and 1,650°C. The data of V activity and oxygen potential were reported, and the oxygen potential was controlled by adjusting the composition of the gas mixture.

Figure 2 shows the comparison of the calculated $VO_{1.5}$ activities in various slags by the GCA model with the experimental measurements. Apart from the data from Shin et al. [7], there is reasonably good agreement between the model calculation and the experimental measurements over several magnitudes range of $VO_{1.5}$ activities. The data from Shin et al. [7] were systematically underestimated. As mentioned above, the oxygen potential in their study could only be calculated based on the [Fe]/(FeO) equilibrium although the FeO content in slag was very low. The high uncertainty of oxygen potential might impact the calculated $VO_{1.5}$ activities. In spite of this, the close agreement between the calculated results and the published data reflects that GCA model basically has a high reliability for describing the multi-

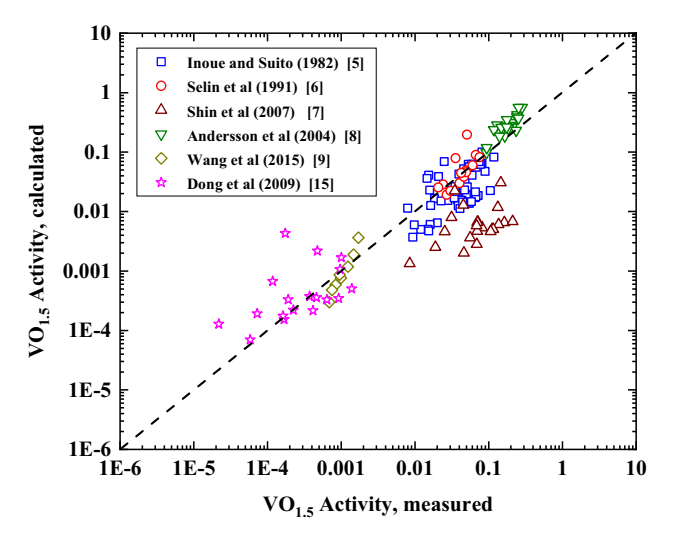


Figure 2: Comparison of the calculated $VO_{1.5}$ activities in various slags by GCA model with the experimental measurements [5–9,15].

component V-containing slags within a wide range of operating conditions.

4 Thermodynamic analysis of V distribution behavior between slag and hot metal

4.1 Analysis of VTM smelting BF operating data

The first stage of V extraction from VTM is to reduce V into hot metal in the BF operation. In this study, the operating data of VTM smelting BF were collected from Pangang Group Xichang Steel & Vanadium Co. Ltd. over a period of 1 year (2021-2022). The VTM smelting BF with an inner volume of 1,750 m³ operated at a productivity of 2.4 $t \cdot (m^{-3} \cdot day^{-1})$, and the slag rate was about 550 kg·t⁻¹. The average coke and coal consumption rates were maintained at 450 and 100 kg·t⁻¹, respectively. The temperature of hot metal was in the range of 1,405-1,495°C, with an average of approximately 1,455°C. Figures 3 and 4 show the compositions of slag and hot metal produced over the 1 year. Here, the V₂O₅ content is only used to denote the V content in the slag. The V₂O₅ content in the slag varied from 0.2 to 0.4 wt%, and the V content in the hot metal was between 0.3 and 0.4 wt%. The compositions of slag and hot metal are listed in Table 2. According to the slag rate and the average compositions, it was calculated that more than 90 wt% of the total charged V in the slag was reduced into the hot metal, while the balance remained in the slag. The TiO₂ content in the slag could reach above 20 wt%, and the exorbitant TiO2 content might promote the formation of Ti carbonitride to largely increase the slag viscosity. The MgO and Al₂O₃ contents in the slag remained at around 9.5 and 14.5 wt%, respectively. A moderate amount of MgO and Al₂O₃ in the slag could balance the slag basicity and improve the slag flowability to promote the reactions between slag and hot metal.

4.2 Thermodynamics of V reduction

V in VTM can be reduced by C to generate metallic V and dissolve into hot metal. V in BF slags is expected to be existed as V_2O_3 dominantly given the strong reducing condition in BF hearths. Assuming that the reactions

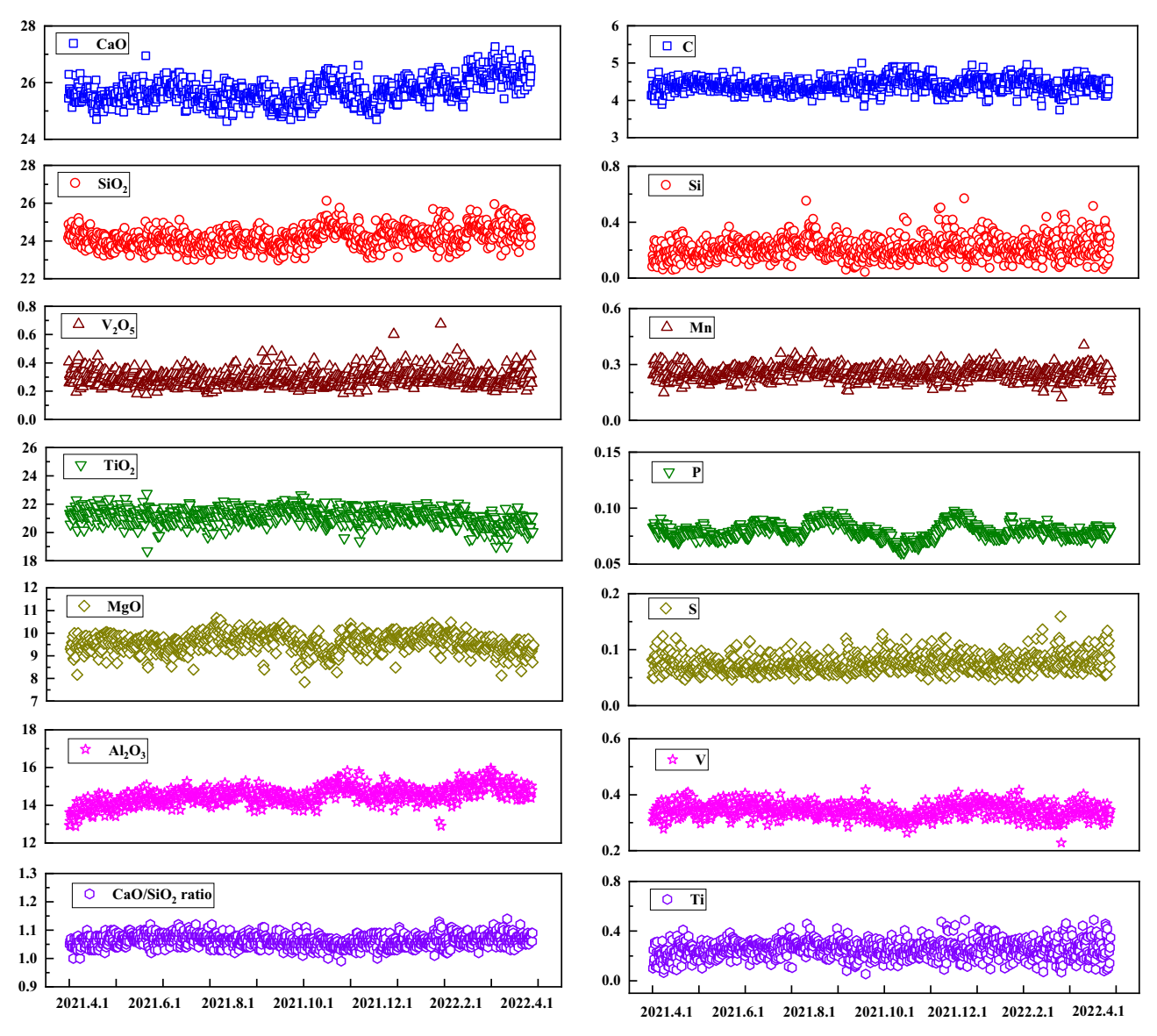


Figure 3: Composition (wt%) of slag produced in the VTM smelting BF over the 1 year (2021–2022).

Figure 4: Composition (wt%) of hot metal produced in the VTM smelting BF over the 1 year (2021–2022).

occurring in BF hearths are close to equilibrium, the reduction of V_2O_3 between the interface of slag and hot metal can be described as the following reaction [17]:

$$\frac{1}{2}(V_2O_3)_{(1)} + \frac{3}{2}[C] = [V] + \frac{3}{2}CO_{(g)},$$

$$\Delta G^{\theta} = -185,815 + 59.74T (J \cdot mol^{-1}).$$
(8)

The corresponding equilibrium constant K_1 of the reaction can be described as the following equation:

$$K_{1} = \frac{(f_{\%,V} \cdot [\%V]) \cdot (P_{CO}/P^{\theta})^{\frac{3}{2}}}{(\gamma_{V_{2}O_{3}} \cdot x_{V_{2}O_{3}})^{\frac{1}{2}} \cdot (f_{\%,C} \cdot [\%C])^{\frac{3}{2}}},$$
(9)

where $f_{\%,V}$, $f_{\%,C}$, and $\gamma_{V_2O_3}$ are the activity coefficients of V and C in hot metal and V_2O_3 in slag, respectively; [%V] and [%C] are the mass fractions of V and C in hot metal; P_{CO} is the equilibrium partial pressure of CO; P^{θ} is the standard gas pressure; and $x_{V_2O_3}$ is the mole fraction of V_2O_3 in slag. The equilibrium partial pressure of CO in BF is usually assumed close to 1 atmosphere at the interface of slag and hot metal phases [18]. In order to calculate the V distribution ratio between slag and hot metal, the methods for determining the activity coefficients of V and C in hot metal and V_2O_3 in slag are described in the following.

Table 2: Composition	s of slag and	hot metal in	the VTM	smelting BF
----------------------	---------------	--------------	---------	-------------

Slag							Hot metal							
Composition	CaO	SiO ₂	V ₂ O ₅	TiO ₂	MgO	Al ₂ O ₃	С	Si	Mn	Р	S	٧	Ti	
Ave./wt%	25.7	24.1	0.31	21.1	9.57	14.5	4.41	0.21	0.25	0.08	0.08	0.34	0.25	
Min./wt%	24.6	23.0	0.18	18.7	7.84	12.9	3.74	0.04	0.12	0.06	0.05	0.23	0.05	
Max./wt%	27.3	26.1	0.68	22.8	10.58	16.0	5.00	0.57	0.40	0.10	0.16	0.42	0.49	

The activity coefficients of V and C in hot metal can be obtained using Wagner's model, which has been widely used for calculating the activity coefficients of elements in alloy phases [19]. The activity coefficients $f_{\%,V}$ and $f_{\%,C}$ can be determined by the following equations:

$$\log f_{\%,V} = \sum e_V^i [\% i], \qquad (10)$$

$$\log f_{\%,C} = \sum e_{\rm C}^{i} [\% i], \tag{11}$$

where $e_{\rm V}^i$ and $e_{\rm C}^i$ are the interaction coefficients, and [%i] represents the mass fractions of elements in hot metal. Table 3 lists the interaction parameters used for calculating the interaction coefficients.

The activity coefficient of V_2O_3 in slag can be calculated by GCA model with a broad range of oxide species: SiO_2 , Al_2O_3 , FeO, Fe_2O_3 , MnO, MgO, CaO, Na_2O , K_2O , P_2O_5 , TiO_2 , T_2O_3 , CrO, Cr_2O_3 , V_2O_3 , V_2O_5 , and other minors. The reliability of describing the multi-component V-containing slag system by GCA model has been evaluated through comparing the calculated V activities with the published experimental measurements in the above.

4.3 Effects of operating conditions on V distribution between slag and hot metal

The V distribution ratio between slag and hot metal $L(V)_{S-HM}$ is defined as the following equation:

$$L(V)_{S-HM} = \frac{(\%V)_{\text{slag}}}{[\%V]_{\text{hot metal}}},$$
(12)

where $(\%V)_{slag}$ and $[\%V]_{hot\ metal}$ represent the mass fractions of V in slag and hot metal, respectively. The plant

measurement of $L(V)_{S-HM}$ under various operating conditions was determined using the operating data of VTM smelting BF shown in Figures 3 and 4. At the same time, with GCA model and the comprehensive slag database in MPE, the impact of each individual operating condition on $L(V)_{S-HM}$ was simulated and evaluated by retaining the other conditions constant at the average compositions shown in Table 2. As shown in Figure 5, the calculated results were compared with the corresponding plant measurements under similar conditions. The calculated trend was confirmed by the plant data although the plant data are quite scattered due to the fluctuation of the operating conditions and slag and hot metal chemistries from heat to heat. The calculated results can help quantifying the impact of each individual operating condition.

Figure 5(a) shows the variation of $L(V)_{S-HM}$ as a function of temperature. The value of $L(V)_{S-HM}$ drops with increasing temperature because the equilibrium constant of V_2O_5 reduction reaction K_1 has a positive correlation with temperature. It means that raising smelting temperature thermodynamically favors more V retain in the hot metal. In actual production, however, the average hot metal temperature of the VTM smelting BF is lower than that of a conventional BF. The reason for lowering the temperature is to lessen the reduction of TiO_2 and then to limit the formation of high-melting Ti carbonitride. The high-melting compound can dramatically enhance the viscosity of slag and make the separation of slag and hot metal more difficult.

Figure 5(b) shows the variation of $L(V)_{S-HM}$ as a function of CaO/SiO₂ ratio. The CaO/SiO₂ ratio in the BF slag is basically between 1.02 and 1.12. Both the calculated results and plant data confirm that the value of

Table 3: Values of interaction parameters

Elements	С	Si	Mn	Р	S	Ti	V
e_V^i	-0.34	0.042	0.05	-0.008	-0.028	_	0.015
$oldsymbol{e}_{\mathcal{C}}^{i}$	0.14	0.08	-0.012	0.051	0.046	0.08	-0.077

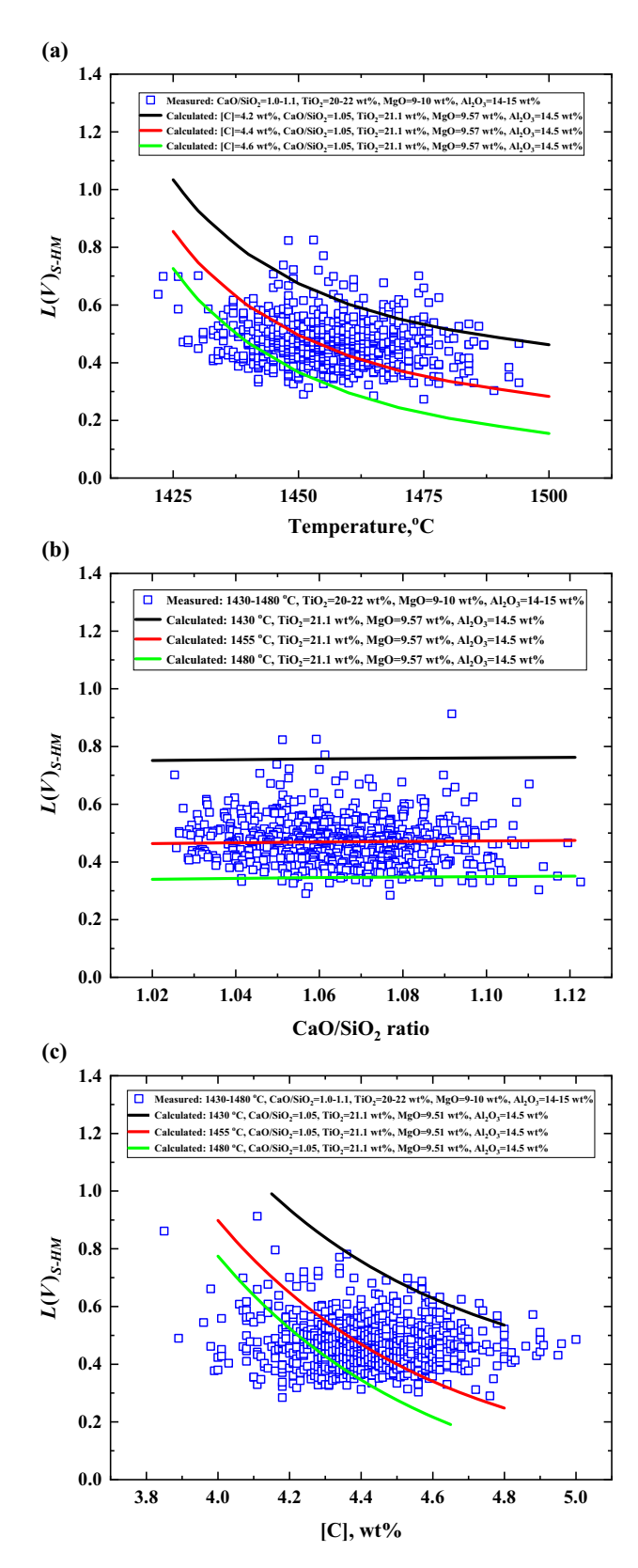


Figure 5: Variation of V distribution ratio between slag and hot metal $L(V)_{S-HM}$ as a function of (a) temperature, (b) CaO/SiO₂ ratio, and (c) C content in hot metal.

 $L(V)_{S-HM}$ is not sensitive to the narrow range of CaO/SiO₂ ratio in the BF slag. Even so, a slight rise of $L(V)_{S-HM}$ with the increasing CaO/SiO₂ ratio can be found according to the calculated results. The study by Inoue and Suito showed that there was a positive correlation between $V^{5+}/(V^{3+} + V^{4+})$ and basicity in the V-containing slag, which means that V transforms to high valence with the increase in basicity. The increase proportion of V^{5+} will reduce the activity of V in slag since the interaction between basic oxide CaO and acid oxide V_2O_5 is strong, which is not beneficial to the reduction of V into hot metal.

Figure 5(c) shows the variation of $L(V)_{S-HM}$ as a function of C content in the hot metal. The calculated results indicate an obvious decline trend with increasing C content, while the trend in plant data is not that obvious. The measured plant data were obtained under the various conditions. The temperature with a range of 1,430-1,480°C may influence/mask the relation between $L(V)_{S-HM}$ and the C content in the hot metal. According to the thermodynamic analysis, the effect of C content in hot metal on $L(V)_{S-HM}$ mostly results from variations of the activity coefficients $f_{\%,V}$ and $f_{\%,C}$. As shown in Table 3, the interaction parameter between C and V is negative, while the selfinteraction parameter of C is positive. Thus, the increasing C content in hot metal can reduce the value of $f_{\%,V}$ but raise that of $f_{\%,C}$, which further leads to the decrease of $L(V)_{S-HM}$. It suggests that increasing the C content in hot metal could be an effective measure to raising the reduction of V into hot metal.

5 Thermodynamic analysis of V distribution behavior between slag and semi-steel

5.1 Analysis of V-recovering BOF operating data

The duplex melting process of BOF is adopted for the steelmaking with V-containing hot metal. First, the V-containing hot metal is selectively oxidized in the BOF operation to cause the V re-distributing between slag and semi-steel, and the V-rich slag can be used in further treatment to recover V in the form of various chemicals. Then, the semi-steel is used for the conventional BOF steelmaking process to reduce carbon content and increase temperature. Likewise, the operating data of V-recovering BOF

were collected from Pangang Group Xichang Steel & Vanadium Co. Ltd. over a period of 1 year (2021–2022). This steel plant has two 200 t BOFs for V extraction and two 200 t BOFs for steelmaking. The average temperature of input hot metal

10 □ CaO 5 n 24 SiO, 18 12 6 32 △ V₂O₅ 24 16 20 TiO, 15 10 10 ♦ MgO 5 Al₂O₃ 16 MnO 12 60 FeO 40 20 0.8 CaO/SiO2 ratio 0.4 0.0 2021.4.1 2021.6.1 2021.8.1 2021.10.1 2021.12.1 2022.2.1 2022.4.1

Figure 6: Composition (wt%) of slag produced in the V-recovering BOF over the 1 year (2021–2022).

was 1,300°C. The temperature of output semi-steel was in the range of 1,320–1,410°C, with an average of 1,360°C. Figures 6 and 7 show the compositions of final V-rich slag and semi-steel over the 1 year. The oxygen was blown into the hot metal to oxidize V and form slag with 12–22 wt% V_2O_5 and semi-steel with less than 4 wt% C. Table 4 lists the compositions of slag and semi-steel. Compared with the composition of hot metal in Table 2, the elements of C, V, Ti, and Mn were oxidized in different degrees. In the V extraction process, the oxidation of elements will release a large amount of heat to make the temperature of molten bath increase rapidly. When the temperature for the oxidation of C and V, the massive oxidation of C will restrain the

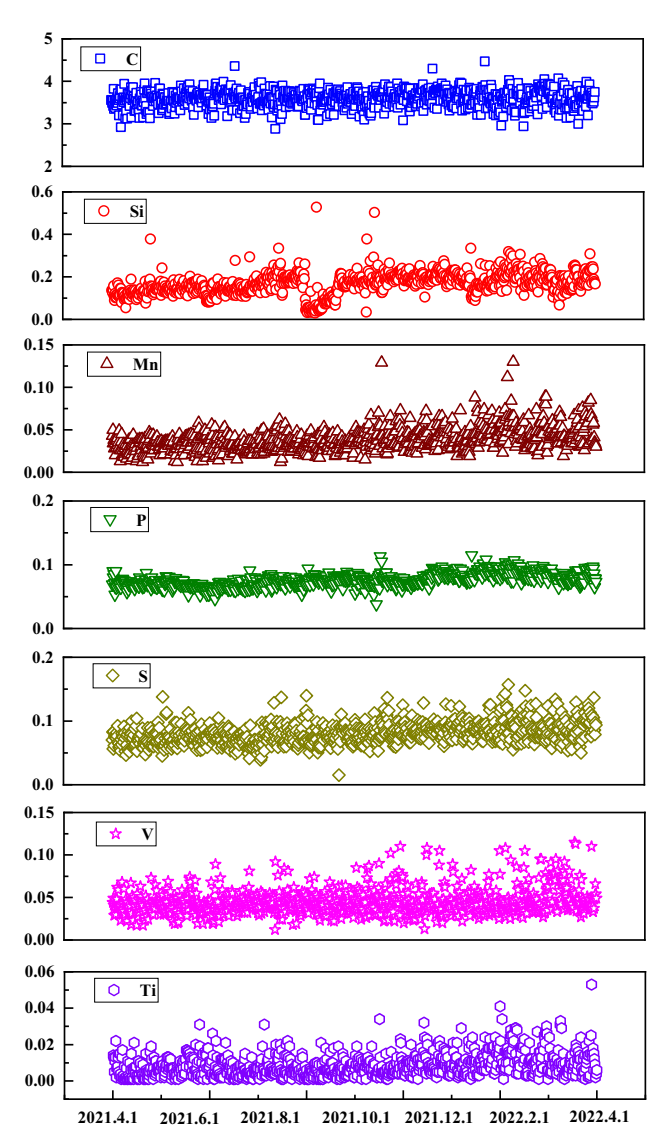


Figure 7: Composition (wt%) of semi-steel produced in the V-recovering BOF over the 1 year (2021–2022).

oxidation of V. Thus, the temperature should be controlled by adding cold charge to delay the C–O reaction.

5.2 Thermodynamics of V oxidation

V in hot metal can be oxidized by FeO to generate V oxides and dissolve into slag phase. V may exist in various forms in oxide phases depending on oxygen potential, temperature, composition, etc. According to the previous studies [20-22], V³⁺ should be the predominant V oxidation state for the slag saturated with metal iron because the oxygen potential and the basicity are relatively low in this situation. Assuming that the reactions occurring at the interface of slag and semi-steel are close to equilibrium, the extraction of V can be described as the following reaction [23]:

$$2[V] + 3(FeO)_{(s)} = (V_2O_3)_{(s)} + 3[Fe],$$
 (13)
 $\Delta G^{\theta} = -390,480 + 149.58T (J·mol-1).$

The corresponding equilibrium constant K_2 of the reaction can be described as the following equation:

$$K_2 = \frac{y_{V_2O_3} \cdot x_{V_2O_3} \cdot a_{Fe}^3}{(f_{\%,V} \cdot [\%V])^2 \cdot (y_{FeO} \cdot x_{FeO})^3},$$
 (14)

where $f_{\%,V}$, γ_{FeO} , and $\gamma_{\text{V}_2\text{O}_3}$ are the activity coefficients of V in semi-steel and FeO and V₂O₃ in slag, respectively; $x_{\text{V}_2\text{O}_3}$ and $x_{\text{V}_2\text{O}_3}$ are the mole fractions of V₂O₃ and FeO in slag; α_{Fe} is the activity of Fe in semi-steel; and [%V] is the mass fraction of V in semi-steel. The value of $f_{\%,V}$ in semi-steel can be determined by Wagner's model as mentioned above, and those of γ_{FeO} and $\gamma_{\text{V}_2\text{O}_3}$ calculated by GCA model and the comprehensive slag database in MPE.

5.3 Effects of operating conditions on V distribution between slag and semisteel

The V distribution ratio between slag and semi-steel $L(V)_{S-SS}$ is defined as the following equation:

$$L(V)_{S-SS} = \frac{(\%V)_{\text{slag}}^{\star}}{[\%V]_{\text{semi-steel}}},$$
(15)

where $(\%V)_{\text{slag}}^{\star}$ and $[\%V]_{\text{semi-steel}}$ represent the mass fractions of V in final V-rich slag and semi-steel, respectively. The plant measurement of $L(V)_{S-SS}$ under various operating conditions was determined using the operating data of V-recovering BOF shown in Figures 6 and 7. Similarly, the impact of each individual operating condition on $L(V)_{S-SS}$ was simulated and evaluated by retaining the other conditions constant at the average compositions shown in Table 4, using GCA model and the comprehensive slag database in MPE. Figure 8 shows the comparison between the calculated results and the corresponding plant measurements under similar conditions. The calculated results could reproduce the variation of $L(V)_{S-SS}$ with slag temperature and composition.

Figure 8(a) shows the variation of $L(V)_{S-SS}$ as a function of temperature. Like the variation trend shown in Figure 5(a), the value of $L(V)_{S-SS}$ at the stage of making V-rich slag also drops with increasing temperature. It reflects that operating at low temperature benefits removing more V into the slag phase. In addition, the purpose of keeping the temperature relatively low at this stage is to preserve the C in the semi-steel as much as possible while oxidizing V into the slag at the same time. According to the Ellingham diagram, V_2O_3 can be reduced to V metal by C at 1,400°C and above. As a result, keeping the temperature under 1,400°C is expected to minimize the reduction of V_2O_3 to V metal by C.

Figure 8(b) shows the variation of $L(V)_{S-SS}$ as a function of CaO/SiO₂ ratio. The value of $L(V)_{S-SS}$ decreases with the increasing CaO/SiO₂ ratio, which agrees with the plant data. This trend is opposite to the trend shown in Figure 8(b) for the BF operation. The difference should be due to the significant difference in the chemistry of BF slag and V-rich slag. By comparison, the CaO/SiO₂ ratio in the V-rich slag is much lower than that in the BF slag. As mentioned above, $V^{5+}/(V^{3+} + V^{4+})$ has a positive correlation with basicity, and thus, V^{3+} should be the predominant V oxidation state for V-rich slag saturated with semi-steel. In this situation, the increase in basicity will raise the activity coefficient of V_2O_3 $\gamma_{V_2O_3}$, which results in

Table 4: Compositions of slag and semi-steel in the V-recovering BOF

Slag							Semi-steel								
Composition	CaO	SiO ₂	V ₂ O ₅	TiO ₂	MgO	Al ₂ O ₃	MnO	FeO	С	Si	Mn	Р	S	٧	Ti
Ave./wt%	2.13	13.3	15.3	11.7	1.81	1.96	8.00	34.1	3.59	0.17	0.04	0.08	0.08	0.05	0.010
Min./wt%	0.47	8.84	9.39	7.91	1.05	1.02	6.09	22.5	2.88	0.03	0.01	0.04	0.02	0.01	0.001
Max./wt%	8.49	21.0	21.8	16.7	7.78	7.12	11.4	42.3	4.47	0.53	0.13	0.12	0.16	0.12	0.053

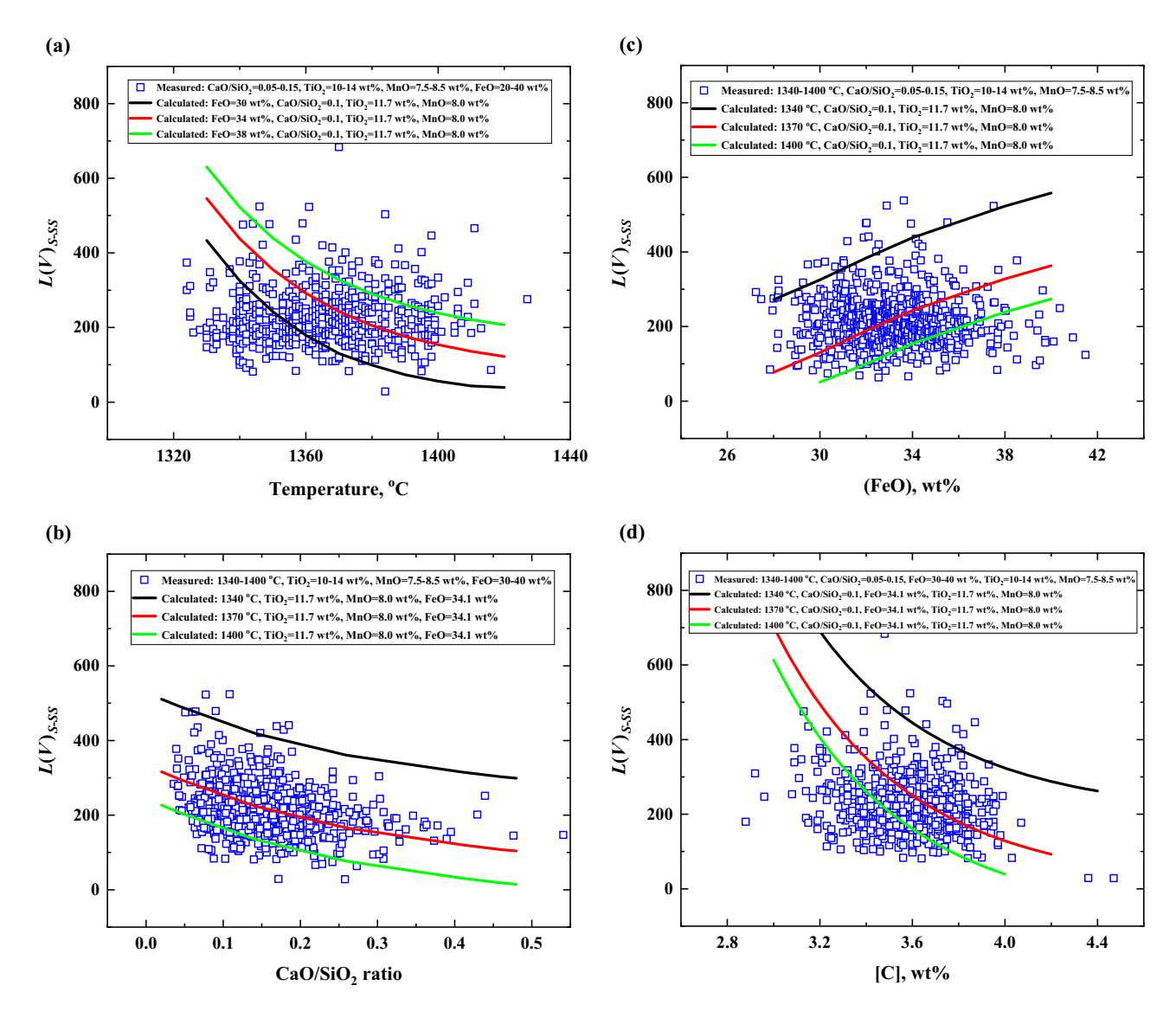


Figure 8: Variation of V distribution ratio between slag and semi-steel $L(V)_{S-SS}$ as a function of (a) temperature, (b) CaO/SiO₂ ratio, (c) FeO content in V-rich slag, and (d) C content in semi-steel.

the decrease of $L(V)_{S-SS}$ according to the thermodynamic analysis. Therefore, an appropriate decrease in basicity will benefit the oxidation of V into V-rich slag phase for the BOF operation.

Figure 8(c) shows the variation of $L(V)_{S-SS}$ as a function of FeO content in the V-rich slag, and the value of $L(V)_{S-SS}$ goes up with the increasing FeO content. As the oxidant for the V oxidation reaction, the increase of FeO content in slag will raise the activity of FeO; hence, we increase the oxygen potential to promote the oxidization of V into slag. In addition, there is a strong interaction between FeO and V_2O_3 , and FeO tends to combine with V_2O_3 to form the spinel Fe₂ V_2O_4 . Therefore, the increase

of FeO can also reduce the activity of V_2O_3 , which favors the V oxidation reaction.

Figure 8(d) shows the variation of $L(V)_{S-SS}$ as a function of C content in the semi-steel. Similar to the variation trend shown in Figure 5(c), the value of $L(V)_{S-SS}$ decreases with increasing C content. Even so, the C in the semi-steel should be preserved as much as possible during the V oxidation process. This is because that the C oxidation is a strong exothermic reaction to largely increase the temperature of molten bath. If the temperature exceeds the critical value, the excessive temperature will further enhance the C oxidation but weaken the V oxidation. Generally, the C content in the semi-steel is controlled around 3.6 wt%.

6 Conclusions

DE GRUYTER

GCA model was applied for analyzing V distribution behavior between slag and hot metal/semi-steel. The calculated VO_{1.5} activities by GCA model were compared with the published experimental measurements to evaluate the reliability of describing the multi-component Vcontaining slag systems. The overall fits by GCA model were satisfactory, and GCA model was capable of simulating the complex high-order slag systems within a wide range of operating conditions.

Production data from a VTM smelting BF ironmaking plant and a V-recovering BOF shop were collected over a period of 1 year. The effects of operating conditions on V distribution ratios between slag and hot metal/semi-steel were analyzed using GCA model. The model calculation could reproduce the variation trend of V distribution ratio with slag temperature and chemistry although the plant data are quite scattered due to the fluctuation of the operating conditions. The simulated results could help quantifying the impact of each individual operating condition and provided the guidance for operators to control V distribution ratios for the better process operation.

The values of $L(V)_{S-SS}$ in the BF operation and $L(V)_{S-SS}$ in the BOF operation both dropped with increasing temperature. In the VTM smelting process, although raising smelting temperature thermodynamically favors more V retain in the hot metal, the average hot metal temperature of the VTM smelting BF is lower than that of a conventional BF to limit the formation of the high-melting Ti carbonitride. In the V-rich making process, operating at low temperature not only benefits distributing more V into the slag phase but also minimizes the reduction of V_2O_3 by C to V in metal.

The value of $L(V)_{S-SS}$ decreased with increasing CaO/ SiO₂ ratio in the BOF operation, which was opposite to the variation trend of $L(V)_{S-HM}$ in the BF operation. The difference is due to the significant difference in the chemistry of BF slag and V-rich slag and the combined effect of interaction between major components. An appropriate decrease in basicity will benefit the oxidation of V into Vrich slag phase for the BOF operation.

Funding information: The authors gratefully acknowledge the financial support by the Fundamental Research Funds for the Central Universities (FRF-TP-20-104A1).

Author contributions: Yang He: methodology, investigation, writing-original draft preparation; Chunlin Chen: conceptualization, formal analysis, writing-review and editing; Xiaodong Yang: Data curation, visualization, software.

Conflict of interest: The authors state no conflict of interest.

Data availability statement: The raw and processed data required to reproduce these findings cannot be shared at this time as the data also forms part of an ongoing study.

References

- Moskalyk, R. R. and A. M. Alfantazi. Processing of vanadium: A review. Minerals Engineering, Vol. 16, No. 9, 2003, pp. 793-805.
- Gilligan, R. and A. N. Nikoloski. The extraction of vanadium [2] from titanomagnetites and other sources. Minerals Engineering, Vol. 146, 2020, id. 106106.
- Yuan, R., S. L. Li, Y. S. Che, J. L. He, J. X. Song, and B. Yang. A critical review on extraction and refining of vanadium metal. International Journal of Refractory Metals and Hard Materials, Vol. 101, 2021, id. 105696.
- Lee, J.-C., Kurniawan, E.-Y. Kim, K. W. Chung, R. Kim, and [4] H.-S. Jeon. A review on the metallurgical recycling of vanadium from slags: Towards a sustainable vanadium production. Journal of Materials Research and Technology, Vol. 12, 2021, pp. 343-364.
- Inoue, R. and H. Suito. Distribution of vanadium between liquid iron and MgO saturated slags of the system CaO-MgO-FeOx-SiO₂. Transactions of the Iron and Steel Institute of Japan, Vol. 22, 1982, pp. 705-714.
- Selin, R. Studies on MgO solubility in complex steelmaking slags in equilibrium with liquid iron and distribution of phosphorus and vanadium between slag and metal at MgO saturation. Scandinavian Journal of Metallurgy, Vol. 20, 1991, pp. 279-299.
- Shin, D. Y., C. H. Wee, M. S. Kim, B. D. You, J. W. Han, [7] S. O. Choi, et al. Distribution behaviour of vanadium and phosphorus between slag and molten steel. Metals And Materials International, Vol. 13, 2007, pp. 171-176.
- Andersson, A. J., M. T. Andersson, and P. G. Jonsson. A study of some elemental distributions between slag and hot metal during tapping of the blast furnace. Steel Research International, Vol. 75, 2004, pp. 294-301.
- [9] Wang, Z., J. Zhang, X. Xing, and Z. Liu. Distribution behaviours and thermodynamic analysis of vanadium between molten iron and high titanium slag. The Chinese Journal of Nonferrous Metals, Vol. 25, 2015, pp. 1355-1361.
- Jung, I.-H. Overview of the application of thermodynamic [10] databases to steelmaking processes. CALPHAD, Vol. 34, 2010, pp. 332-362.
- Lehmann, J., F. Bonnet, and M. Bobadilla. Thermodynamic description of liquid steel and metallurgical slags by the generalized central atom model. AIST Transactions, Vol. 3, 2006, pp. 114-123.

- [12] Lehmann, J. Application of ArcelorMittal Maizières thermodynamic models to liquid steel elaboration. *Revue de Metallurgie* (*Les Ulis, France*), Vol. 105, 2008, pp. 539–550.
- [13] Chen, C. L., L. Zhang, and J. Lehmann. Thermodynamic modelling of phosphorus in steelmaking slags. *High Temperature Material Processes*, Vol. 32, No. 3, 2013, pp. 237–246.
- [14] He, Y., C. L. Chen, and J. Lehmann. Thermodynamic modeling of CaO-SiO₂-VO_x system by the generalized central atom model. CALPHAD, Vol. 76, 2022, id. 102366.
- [15] Dong, P., X. Wang, and S. Seetharaman. Activity of VO1.5 in CaO-SiO2-MgO-Al2O3 slags at low vanadium contents and low oxygen pressures. Steel Research International, Vol. 80, 2009, pp. 251–255.
- [16] Sigworth, G. K. and J. F. Elliott. The thermodynamics of liquid dilute iron alloys. *Metal Science*, Vol. 8, 1974, pp. 298–310.
- [17] Zhang, B. H., Q. C. Liu, C. W. Li, D. Y. Zou, and J. B. Sun. Thermodynamics of V reduction in smelting reduction slag for vanadium-titanium-containing magnetite. *Acta Metallurgica Sinica*, Vol. 29, No. 5, 1993, pp. 193–199.
- [18] Shankar, A. Sulphur partition between hot metal and high alumina blast furnace slag. *Ironmak. Steelmak*, Vol. 33, 2006, pp. 413–418.

- [19] Andersson, M. A., P. G. Jonsson, and M. M. Nzotta. Application of the sulphide capacity concept on high-basicity ladle slags used in bearing-steel production. *ISIJ International*, Vol. 39, 1999, pp. 1140–1149.
- [20] Wright, S. and S. Jahanshahi. A review of Vanadium redox reactions in melts. 6th Conference of the Asia Pacific Confederation of Chemical Engineering, Institution of Engineers, Australia, Barton, ACT, 1993, pp. 359–363.
- [21] Vermaak, M. K. G. and P. C. Pistorius. Equilibrium slag losses in ferrovanadium production. *Metallurgical and Materials Transactions B: Process Metallurgy and Materials Processing Science*, Vol. 31B, 2000, pp. 1091–1097.
- [22] Farah, H. and M. Brungs. Oxidation-reduction equilibria of vanadium in CaO-SiO₂, CaO-Al₂O₃-SiO₂ and CaO-MgO-SiO₂ melts. *Journal of Materials Science*, Vol. 38, 2003, pp. 1885–1894.
- [23] Zhen, X. P., B. Xie, C. Y. Zhao, and Q. Y. Huang. Vanadium distribution behavior at the end point of vanadium extraction by converter process. *Journal of University of Science and Technology Beijing*, Vol. 34, No. 12, 2012, pp. 1371–1378.